IS-PORTO 2023 PROCEEDINGS

Proceedings of the 8th International Symposium on DEFORMATION CHARACTERISTICS OF GEOMATERIALS Porto, 3rd - 6th September 2023

Acoustic emissions during creep under triaxial compression

Belinda Bock[1#], *Stefan* Vogt[1], and *Roberto* Cudmani[1]

[1]*Technical University of Munich, TUM School of Engineering and Design, Department of Civil and Environmental Engineering, 81245 Munich, Germany*
[#]*Corresponding author: belinda.bock@tum.de*

ABSTRACT

Granular materials exhibit time- and rate-dependent behaviour resulting from micromechanical processes at the scale of individual particles. Elastic energy is released during these processes and can be detected as acoustic emissions (AE). Using multistage creep tests under isotropic and anisotropic pressure on medium dense samples of dry silica sand, the relationship between the number of AE events N_{AE} and the axial creep strain ε_a was determined. In addition, the dependence on the mean pressure p and the deviator stress q was investigated. The experimental results show that the development of AE and axial strain during creep are qualitatively comparable. Within the creep phases both the change in ε_a and N_{AE} can be described by a logarithmic trend with time. The time-dependent development of both measured quantities exhibit a dependence on q. Moreover, the evolution of N_{AE} with time also shows a pronounced increase with increasing p. A time-dependent power law can be assumed to represent the rates of N_{AE} and the rates of ε_a with time during creep. The exponent m of the power law is similar for all experiments performed. The initial rates of N_{AE} and ε_a increase with increasing p as well as increasing q/p-ratio. Finally, a linear correlation between $\log(\dot{\varepsilon}_a)$ and $\log(\dot{N}_{AE})$ was found depending on two state parameters a and b, with a seems to be independent on the stress state.

Keywords: granular material; creep; acoustic emission; triaxial testing

1. Introduction

Granular materials exhibit time- and rate-dependent behaviour. This macroscopic quasi-viscous behaviour is observeable as creep, relaxation and strain rate dependency, respectively. Creep is the time-dependent increase of strain under constant effective pressure. Although the magnitude is much smaller in granular soils compared to fine-grained soils, creep is considered for predicting serviceability regarding certain challenges of geotechnical engineering, such as determining the deformation of artificial fills of significant depth (e.g. Levin et al. 2022).

Creep in granular materials is the result of time-dependent micromechanical processes at the level of particle contacts (microscale) and particle assemblies (mesoscale). Various researchers have already investigated governing time-dependent processes at the micro- and macroscale that occur during creep in granular materials:

- particle translation and rotation (Mejia et al. 1988)
- different degrees of particle fracture and breakage (Brzesowsky et al. 2014; Mesri and Vardhanabhuti 2009)
- micro-interlocking of surfaces (Schmertmann 1991)
- static fatigue of asperities at the particle surface (Michalowski et al. 2018)
- time-dependent buckling of strong force chains along a string of individual particles (Bowman and Soga 2003)

During these time-dependent micromechanical processes elastic energy is released that can be detected by the AE measurement technique. Michlmayr et al. (2012) identify as sources of acoustic emissions, friction between grains due to rotation and translation, crack propagation within individual particles, force-chain buckling, as well as grain fracture and breakage, which correspond to the micromechanical processes involved in creep. The acoustic emission method promises great potential for monitoring and evaluating deformation and failure behaviour of soil and soil-like materials as well as geotechnical structures, as it is non-destructive with real-time triggering. In contrast to other methods, the measurement equipment is comparably simple and, due to increasing as well as cheap storage capacity that allow the measurement of high frequencies, the method also proves to be economical. An example for a geotechnical application for which the acoustic emission method is already being used is the monitoring of slope stability (e.g. Koerner et al. 1981; Shiotani and Ohtsu 1999). Furthermore, the method is also tested successfully to qualitatively determine the stress-strain behaviour and the different patterns of shear planes during triaxial compression tests on silica sand (Lin et al. 2020b; e.g. Smith and Dixon 2019) as well as the compression behaviour of sands in oedometer tests (Fernandes et al. 2010). In contrast to the works that measure AE during loading processes, the monitoring of time-dependent effects of granular materials by the acoustic emission method is not established yet. The relationship between axial creep strain and acoustic emissions under

oedometric conditions was investigated to some extent by Brzesowsky et al. (2014) and Bock et al. (2022). The acoustic emissions that occur during an isotropic and anisotropic consolidation phase of a well graded sand were triggered by Tanaka and Tanimoto (1988). Experiments that trigger acoustic emissions during creep phases at deviator stress close to the maximum of shear resistance are not known to the authors to date. A comprehensive study to determine a relationship between creep deformation and AE for different stress states is therefore missing.

Thus, the paper presents an experimental approach to link the detection of acoustic emissions emitted by the processes inside the specimens to the macroscopically observable creep deformation measured by conventional measurement methods at the sample boundaries. For this purpose, multistage creep tests under isotropic and anisotropic conditions on dry silica sand using a triaxial apparatus were carried out.

2. Material

Dry silica sand as so-called Cuxhaven Geest Sand is used for the experimental investigation, which originates from a sand quarry close to the North See in Germany. The sand quarry is located on a so-called Geest remaining from the last glacial epoch forming a range of hills up to about 30 m above the sea level at the vicinity of Midlum close to the city of Cuxhaven. The grain size distribution of the uniform and narrow graded material is shown in Fig. 1. The material characteristics are given in Table 1.

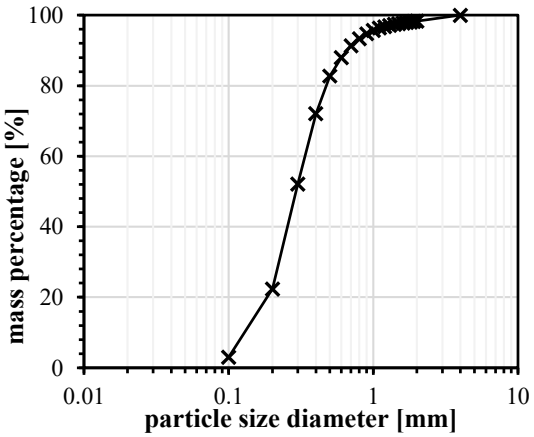

Figure 1. Grain size distribution of Cuxhaven Geest Sand.

3. Description of the test setup, sample preparation and test procedure

3.1. Test setup

For the drained triaxial compression tests, the setup shown in Fig. 2 was used. Linear encoders as displacement transducers with a resolution of 0.025 µm measured the axial creep deformation by logging the displacement of the axial piston outside the pressure chamber. The volume change of the samples during creep was measured by the cell in cell principle as described for example in Lade (2016).

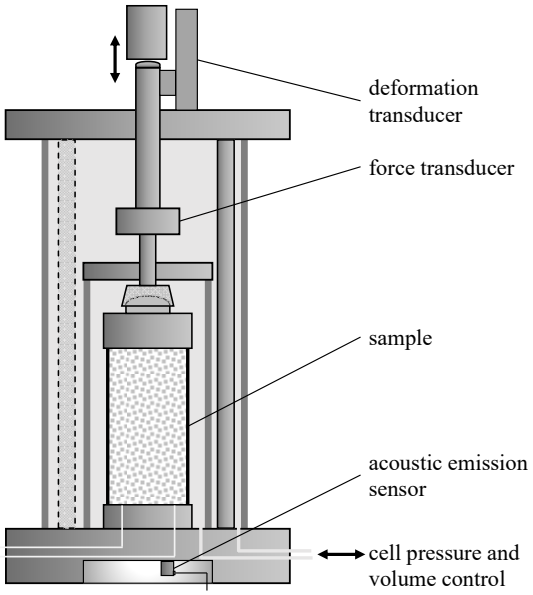

Figure 2. Schematic sketch of the used type of triaxial cell.

The sensor of the acoustic emission measurement was attached below the specimen on the bottom plate. Hot melt adhesive was used as coupling agent. The contact was proven by the pencil lead break test (Vallen 2003). The passive piezoelectric AE sensor, which is sensitive in the frequency range from 20 kHz to 450 kHz, had a peak frequency of 280 kHz. The elastic waves generated during creep were picked up by the sensor and amplified by 34 dB using a preamplifier. The signal was digitalised at a sampling rate of 10 MHz and filtered by a digital band-pass filter ranging from 25 kHz to 300 kHz. The output of the AE measurement is parametric data real time processed from the sensor readings. Bock et al. (2022) describe the used measurement system in detail and explain the controlling parameters for the real time dataprocessing. If the signal exceeds a specific amplitude threshold, it is counted as an acoustic emission event (AE event). Using a dummy specimen made out of PTFE, the amplitude threshold for the experimental setup was determined as 45 dB.

An AE event was defined to end after a rearm time of 204.8 µm, which is the time starting after the signal was finally dropped below the amplitude threshold.

Table 1. Material characteristics of Cuxhaven Geest Sand

Grain density and grain strength		Limiting void ratio		Grain size distribution		
ρ_s [g/cm^3]	Hardness after Mohs	e_{max}	e_{min}	d_{50} [mm]	C_U	C_C
2.62	6.0 to 7.0	0.75	0.48	0.29	2.62	1.14

3.2. Sample preparation

In order to obtain robust measurements of deformation and volume change during creep a comparably large sample dimension was chosen preparing specimens of an initial height of 200 mm and initial diameter of 100 mm. The air pluviation method was applied, which is known to produce homogeneous samples that are comparably close to the structure found in the natural deposit (Lade 2016). Furthermore, the air pluviation method satisfy the high requirements for reproducibility regarding a certain initial void ratio. Medium dense samples with initial relative density I_D in the range of 0.41 – 0.44 were prepared in a sample mold and then put under vacuum to guarantee stability until an initial cell pressure of 50 kN/m^2 was reached.

3.3. Test procedure

Multistage creep tests under isotropic and anisotropic conditions were performed to determine the relationship between acoustic emissions and creep deformation. To investigate isotropic creep, a sample was loaded by an isotropic stress rate of 100 kN/m^2/min up to the initial creep phase at a pressure of p_0 = 500 kN/m^2. The pressure was kept constant for at least 5 days. Subsequently, the pressure was increased to p_0 = 1000 kN/m^2 using the same pressure rate and again kept constant for at least 5 days. The procedure was repeated for a pressure of p_0 = 2000 kN/m^2. In order to study states of anisotropic pressure with a second test series, following the loading up to the above-mentioned pressures p_0, a deviator stress of 0.2 q_{max} was applied by an axial strain rate of 0.1 %/min, while the cell pressure was kept constant. q was subsequently kept constant again at least for 5 days. After further strain-controlled axial loading up to 0.9 q_{max}, a creep phase of a minimum of 5 days was repeated. The test procedure is illustrated by the scheme given by Fig. 3.

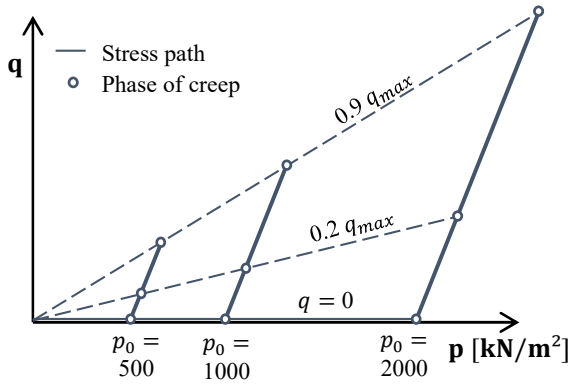

Figure 3. Illustration of the test procedure for conducting creep phases at different pressures p_0 and q.

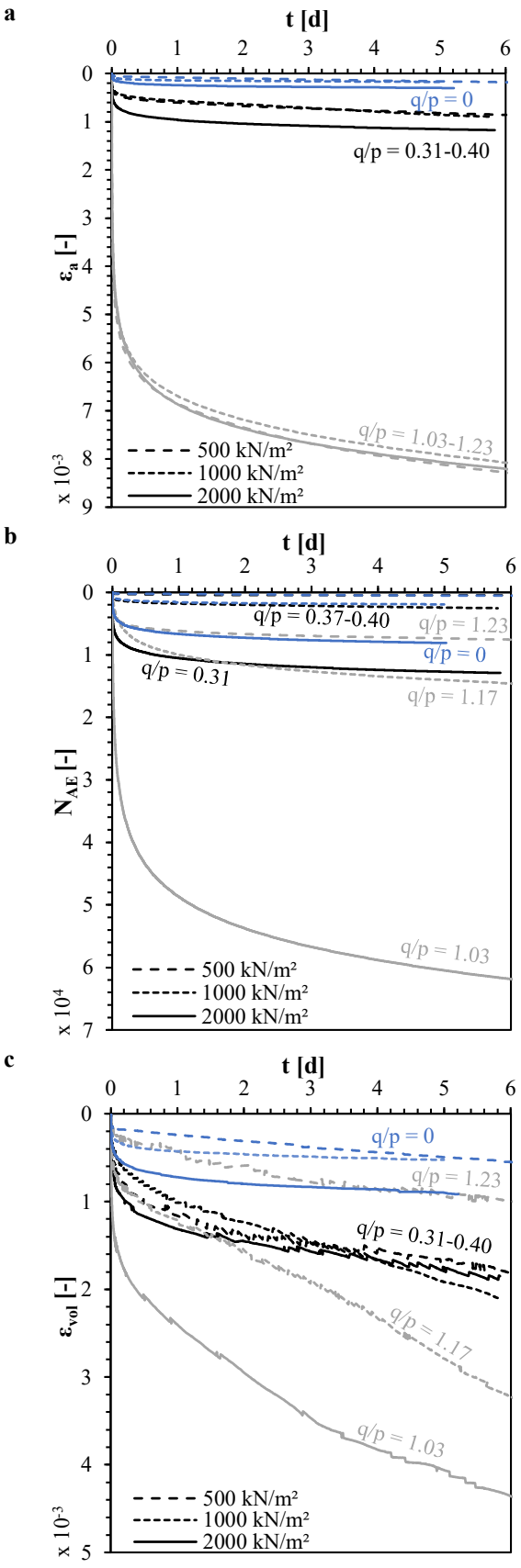

Figure 4. a Axial strain ε_a, **b** number of AE events N_{AE} and **c** volumetric strain ε_{vol} with time t since start of the creep phases at varying p_0 and q/p-ratios.

4. Results

In the following, the results of the measured axial strain ε_a, the volumentric strain ε_{vol} and the cumulated

number of AE events N_{AE} during creep phases at isotropic pressure ($q/p = 0$) and anisotropic pressure of 0.2 q_{max} ($q/p \approx 0.36$) and 0.9 q_{max} ($q/p \approx 1.15$) on samples of Cuxhaven Geest Sand are given. Different types of lines highlight the pressures of p_0 = 500 kN/m², 1000 kN/m² and 2000 kN/m², whereas the differentiation in q/p-ratio is indicated by the variation in color.

In Fig. 4 the evolution of ε_a, N_{AE} and ε_{vol} with time t are presented. It shows that N_{AE} follows qualitatively the same time and pressure dependent trend as ε_a. ε_a and N_{AE} increase with increasing q/p-ratio which is in accordance to the investigations of Tanaka and Tanimoto (1988). Whereas the values of ε_a at same q/p-ratio but different pressure p_0 after 5 days of creep are approximately in the same range, the influence of the pressure p_0 on the number of AE events N_{AE} is visible. A reason for this may be the influence of soil structure, pressure and density on the propagation characteristics of elastic waves as shown by Lin et al. (2020a). With increasing confining pressure or densification process, the travel path of the elastic waves decreases due to the restructuring of the particles (e.g. formation of strong force chains) through the sample to the acoustic emission sensor and in addition, the attenuation of the waves is also reduced due to stiffening at particle contacts. Thus, for the same amplitude threshold, more AE events can be detected as the pressure p_0 increases.

Because of the initially medium dense specimens, the creep phases started in the range of contractive volumetric behaviour. Thus, contractive creep was to be expected (Kuwano and Jardine 2002). The experiments at $q/p \approx 0.36$ show a similar trend regarding the volumetric strain ε_{vol} during creep independent of the pressure p_0, whereas the creep phases at $q/p \approx 1.15$ show a clear dependence on the pressure p_0 resulting in an increasing ε_{vol} with increasing p. Until now by evaluating the available test data we were not able to find a relationship between ε_{vol} and N_{AE}.

In Fig. 5 the curves of ε_a and N_{AE} are additionally shown by using semi-logarithmic scaled diagrams. An almost linear development of ε_a and N_{AE} with log (t) can be assumed after a certain time span at the beginning of the creep phases. Thus, the axial strain ε_a developing during creep can be described by the well-known creep coefficient C (Buisman 1936) as

$$\varepsilon_a - \varepsilon_{a,0} = C \cdot \ln \frac{t_{ref}+t}{t_{ref}}, \quad (1)$$

where t_{ref} represents the point of intersection between the linear slope of the curve and the ln (t)-axis. At t_{ref} the value of $\varepsilon_{a,0}$ is obtained.

The acoustic emission coefficient C_{AE} can be defined analogously as presented in Bock et al. (2022) by

$$N_{AE} - N_{AE,0} = C_{AE} \cdot \ln \frac{t_{ref}+t}{t_{ref}}. \quad (2)$$

Accordingly to Eq. (1), $N_{AE,0}$ represents the number of AE events at t_{ref}.

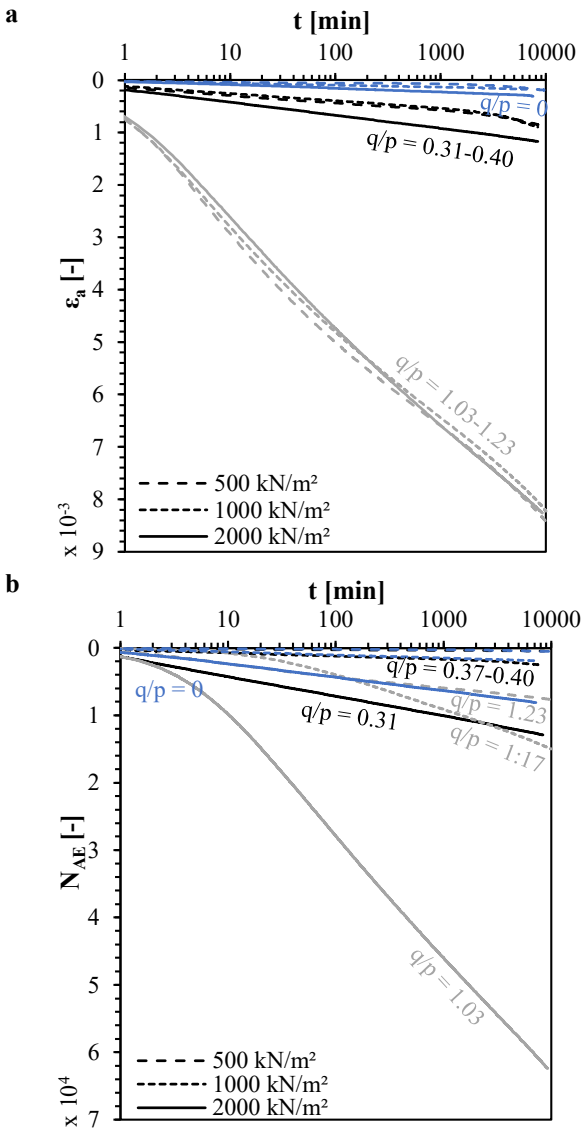

Figure 5. a Axial strain ε_a, **b** number of AE events N_{AE} with log (t) for creep phases at varying p_0 and q/p-ratios.

Furthermore, the axial creep strain rates $\dot{\varepsilon}_a = d\varepsilon_a/dt$ and rates of number of AE events $\dot{N}_{AE} = dN_{AE}/dt$ were calculated and are presented in Fig. 6 regarding time t in a double logarithmic diagram. The relationship between $\dot{\varepsilon}_a$ and $\dot{N}_{AE}$, respectively, and the time t can be well described by an exponential approach.

$$\dot{\varepsilon}_a = t^{-m_{\varepsilon_a}} \quad (3)$$

or

$$\dot{N}_{AE} = t^{-m_{N_{AE}}}, \quad (4)$$

respectively. Concerning the axial strain rate $\dot{\varepsilon}_a$, the exponent m_{ε_a} lies for Cuxhaven Geest Sand in the range of 0.93 to 0.98, being slightly higher for higher q/p-ratios. Similar results are shown for the rate of number of AE events $\dot{N}_{AE}$ with $m_{N_{AE}}$ varying between 0.95 and 0.98. The exponent m_{ε_a} or $m_{N_{AE}}$, respectively, was determined in the range between 10 min and 1000 min, in which the slope of the curves is assumed to be linear using the double logarithmic scale.

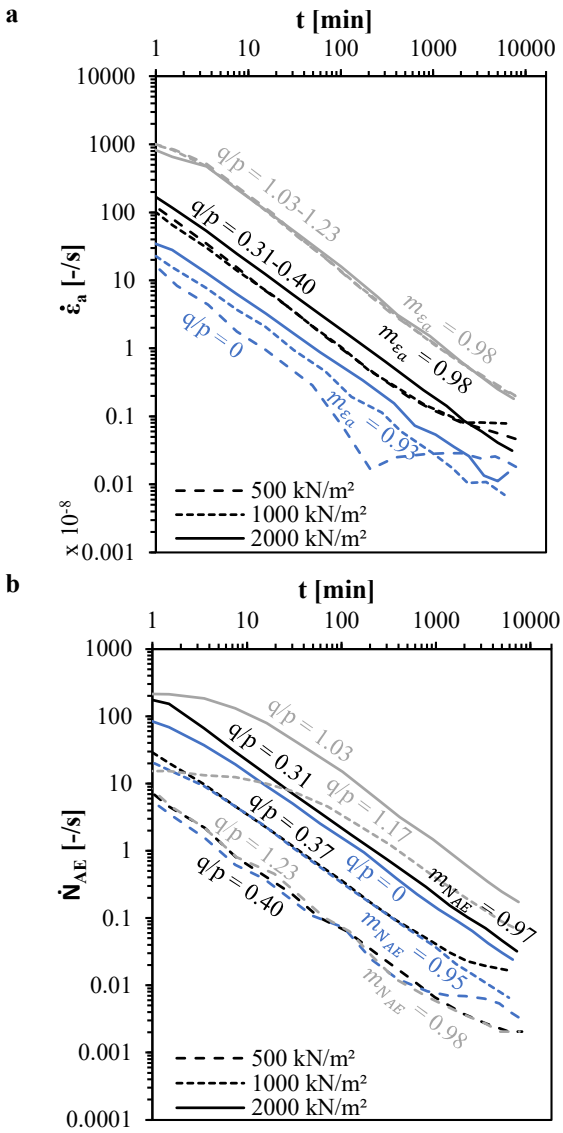

Figure 6. a Axial strain rate $\dot{\varepsilon}_a$, **b** rate of number of AE events $\dot{N}_{AE}$ with time t for creep phases at varying p_0 and q/p-ratios (double logarithmic scale).

Higher values of m indicate a slower decrease of the axial strain rate $\dot{\varepsilon}_a$ or rate of number of AE events $\dot{N}_{AE}$, respectively, and thus, a slower stabilisation process of micromechanical processes during creep within the sample. The sudden change of both $\dot{\varepsilon}_a$ and $\dot{N}_{AE}$ observed during the creep phase at $p_0 = 500$ kN/m² can be explained by a sudden destabilisation process at the particle contacts. Such change of rates was only observed during the first creep stage of the conducted multistage creep tests.

Thus, the stress dependent creep behaviour with time (Fig. 4) appears to correspond to the different initial axial strain rates $\dot{\varepsilon}_a$ or rates of number of AE events $\dot{N}_{AE}$, followed by an almost identical exponential decrease of the rates. Increasing initial rates of $\dot{\varepsilon}_a$ and $\dot{N}_{AE}$ are observed as the deviator stress q increases and, in the case of $\dot{N}_{AE}$, as the mean pressure p increases.

The axial creep strain ε_a and the number of AE events N_{AE} during the creep phases are furthermore compared in Fig. 7 a. The double logarithmic axis of the diagram indicates an approximate linearity between this two measured quantities. The first measured values plotted in the diagram correspond to the time of $t = 10$ s after the creep pressure has been reached. Thereby, the initial axial creep strain $\varepsilon_{a,0}$ is larger for the creep phases with higher q/p-ratio, while the initial number of AE events $N_{AE,0}$ is apparently not follwing a clear trend with respect to the ratio q/p. In contrast, the $N_{AE,0}$ increases with increasing p_0, whereas ε_a is less affected. An exception is measured for creep at $q/p = 1.17$ and $p_0 = 1000$ kN/m², which has initially a lower $N_{AE,0}$ than the experiment at $p_0 = 500$ kN/m². A change of the linear relation between $\log(\varepsilon_a)$ and $\log(N_{AE})$ is notified for samples at $p_0 = 2000$ kN/m² and $q/p > 0.31$ as well as for the test at $p_0 = 1000$ kN/m² and the highest deviator creep stress at a ratio of $q/p = 1.17$. A reason for this behaviour might be the higher value of t_{ref} according to Eq. (1) or Eq. (2), respectively. The deviating time span at the beginning of the creep phase where the linear trend has not been established due to the preceding loading phase is more significant because of the double logarithmic data representation.

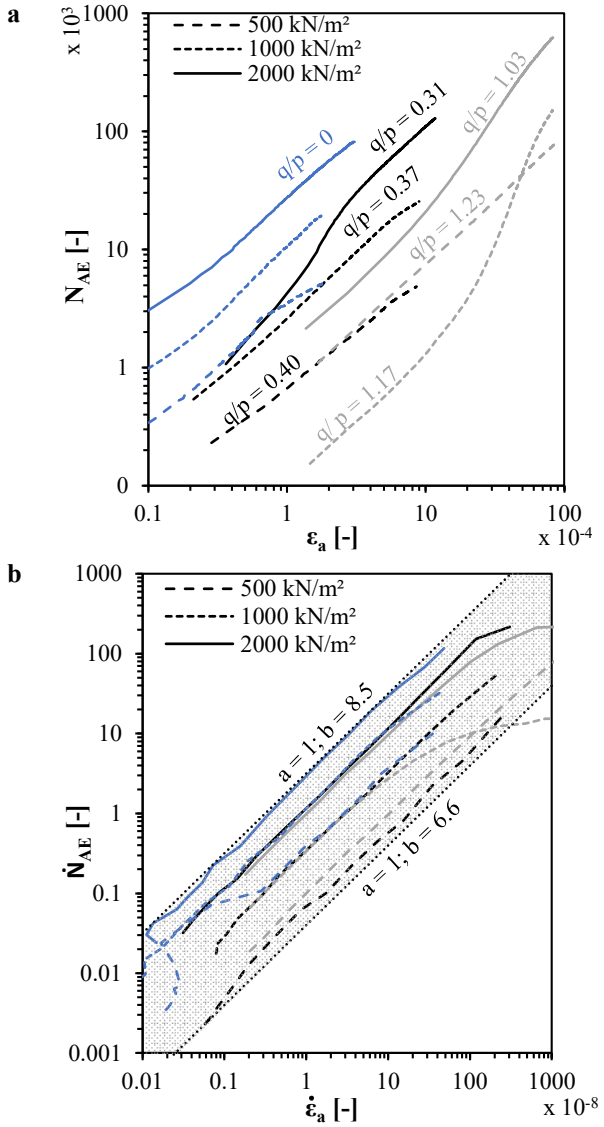

Figure 7. a Axial strain ε_a versus number of AE events N_{AE} and **b** axial strain rate $\dot{\varepsilon}_a$ versus rate of number of AE events $\dot{N}_{AE}$.

In a last diagram of Fig. 7 b, the logarithm of axial strain rate $\dot{\varepsilon}_a$ is compared with the logarithm of the rate of the number of AE events $\dot{N}_{AE}$. Accordingly, we suggest a relationship between $\dot{\varepsilon}_a$ and $\dot{N}_{AE}$ for the investigated material following

$$\dot{N}_{AE} = 10^b \cdot {\dot{\varepsilon}_a}^a, \quad (5)$$

with a and b being parameters specific for the material and probably as well dependent on the initial density. The parameter a is stress state-independent, whereas b has to be determined as a function of p and q. For the investigated ranges of p_0 and q/p, the parameter a can be set to 1.0 for all experiments, whereas b varies in the range of 6.6 to 8.5: With increasing pressure p_0, b increases. Furthermore, b is slightly higher for isotropic compared to anisotropic stress conditions. The experiments at anisotropic stress (q/p-ratio > 0) with constant p_0 show similar values of b.

5. Summary and Conclusion

Multistage creep tests under drained triaxial compression were perfomed on dry, medium dense samples of a silica sand from Cuxhaven, Germany. In addition to isotropically loaded samples in a pressure range between $p_0 = 500$ kN/m² and 2000 kN/m², anisotropic pressure states at about 0.2 q_{max} and 0.9 q_{max} were investigated. The stress paths to achieve the anisotropic states consisted of isotropic compression to the pressure p_0 followed by an increase of q at constant cell pressure. During the creep phases of at least 5 days the axial and volumetric strain during creep was determined in a conventional way using displacement transducers and by measuring the chance of the inner cell fluid according the the triaxial cell in cell principle. In parallel, the number of acoustic emissions exceeding an ambient noise level (amplitude threshold) was counted.

The results demostrate that acoustic emissions originating from micromechanical processes and the axial strain are related during creep. The number of AE events N_{AE} and the axial strain ε_a show a similar evolution with time. Increasing ε_a and N_{AE} were found with increasing p and q/p-ratio. The relationship between ε_a, respectively, N_{AE} with the $\log(t)$ can be described by the creep coefficients C and C_{AE}, which are not constant during the phase of creep. On the contrary, the rates $\dot{\varepsilon}_a$ and $\dot{N}_{AE}$ during creep follow an exponential trend with time, whereby the exponent m_{ε_a} and $m_{N_{AE}}$, respectively, is similar for all conducted tests, but the rates at the onset of the creep phase $\dot{\varepsilon}_{a,0}$ and $\dot{N}_{AE,0}$ increase with p and q/p-ratio.

The linear relationship between $\log(\dot{\varepsilon}_a)$ and $\log(\dot{N}_{AE})$ described by a power law using the parameters a and b suggests that the axial creep strain rate as well as the axial creep strain can be evaluated from the rate of change of the number of AE events. For the conducted experiments the parameter a is stress state-independent, whereas the parameter b depends on the stress state. Both parameters most likely are dependent on the material as well as the density. The found relationship migth be especially useful for the evaluation of creep strain for long creep time, in which the strain becomes very small and the conventional evaluation of strain based on displacement transducers reaches its limit. The relationship and its dependencies shall be evaluated by further experiments.

Acknowledgements

The authors are very thankful for the financial support provided by the German Research Foundation (DFG) [CU363/1-1].

References

Bock, B. A.-M., F. Levin, S. Vogt, and R. Cudmani. "Acoustic Emission of Sand during Creep under Oedometric Compression." *Geotech. Test. J.*, 45(2): 20210007. 2022. https://doi.org/10.1520/GTJ20210007.

Bowman, E. T., and K. Soga. "Creep, ageing and microstructural change in dense granular materials." *Soils Found.*, 43(4): 107–117. 2003. https://doi.org/10.3208/sandf.43.4_107.

Brzesowsky, R. H., S. J. T. Hangx, N. Brantut, and C. J. Spiers. "Compaction creep of sands due to time-dependent grain failure: Effects of chemical environment, applied stress, and grain size." *J. Geophys. Res. Solid Earth*, 119(10): 7521–7541. 2014. https://doi.org/10.1002/2014JB011277.

Buisman, A. S. K. "Results of Long Duration Settlement Tests." *Proceedings of the 1st International Conference on Soil Mechanics and Foundation Engineering*, (I): 103–106. 1936.

Fernandes, F., A. I. Syahrial, and J. R. Valdes. "Monitoring the Oedometric Compression of Sands with Acoustic Emissions." *Geotech. Test. J.*, 33(5): 102501. 2010. https://doi.org/10.1520/GTJ102501.

Koerner, R. M., W. M. McCabe, and A. E. Lord. "Acoustic Emission Behavior and Monitoring of Soils." In: Acoustic Emissions in Geotechnical Engineering Practice, ASTM STP 750, edited by V. P. Drnevich, and R. E. Gray: 93-141, West Conshohocken, PA: ASTM. 1981.

Kuwano, R., and R. J. Jardine. "On measuring creep behaviour in granular materials through triaxial testing." *Can. Geotech. J.*, 39(5): 1061–1074. 2002. https://doi.org/10.1139/t02-059.

Lade, P. V. "Triaxial testing of soils". Wiley Blackwell, Chichester West Sussex United Kingdom. 2016.

Levin, F. C., M. Back, S. Vogt, and R. Cudmani. "Experiment-based estimation of the settlement potential due to dynamic loads from heavy vehicle traffic on the A 44n motorway built on the dump of the Garzweiler opencast mine." *Transportation Geotechnics*, 32: 100674. 2022. https://doi.org/10.1016/j.trgeo.2021.100674.

Lin, W., A. Liu, W. Mao, and J. Koseki. "Acoustic emission behavior of granular soils with various ground conditions in drained triaxial compression tests." *Soils Found.*, 60(4): 929–943. 2020a. https://doi.org/10.1016/j.sandf.2020.06.002.

Lin, W., A. Liu, W. Mao, and J. Koseki. "Acoustic emission characteristics of a dry sandy soil subjected to drained triaxial compression." *Acta Geotech.*, 15(9): 2493–2506. 2020b. https://doi.org/10.1007/s11440-020-00932-w.

Mejia, C. A., Y. P. Vaid, and D. Negussey. "Time dependet behaviour of sand." In: International Conference on Rheology and Soil Mechanics: Proceedings, edited by M. J. Keedwell: 312–326: Spon Press. 1988.

Mesri, G., and B. Vardhanabhuti. "Compression of granular materials." *Can. Geotech. J.*, 46(4): 369–392. 2009. https://doi.org/10.1139/T08-123.

Michalowski, R. L., Z. Wang, and S. S. Nadukuru. "Maturing of contacts and ageing of silica sand." *Géotechnique*, 68(2): 133–145. 2018. https://doi.org/10.1680/jgeot.18.D.004.

Michlmayr, G., D. Cohen, and D. Or. "Sources and characteristics of acoustic emissions from mechanically stressed geologic granular media — A review." *Earth-Sci. Rev.*, 112(3-4): 97–114. 2012. https://doi.org/10.1016/j.earscirev.2012.02.009.

Schmertmann, J. H. "The Mechanical Aging of Soils." *J. Geotech. Eng.*, 117(9): 1288–1330. 1991. https://doi.org/10.1061/(ASCE)0733-9410(1991)117:9(1288).

Shiotani, T., and M. Ohtsu. "Prediction of Slope Failure Based on AE Activity." In: Acoustic Emission: Standards and Technology Update, edited by S. J. Vahaviolos, West Conshohocken, PA: ASTM. 1999.

Smith, A., and N. Dixon. "Acoustic emission behaviour of dense sands." *Géotechnique*, 69(12): 1107–1122. 2019. https://doi.org/10.1680/jgeot.18.P.209.

Tanaka, Y., and K. Tanimoto. "Time Dependent Deformation of Sand as Measured by Acoustic Emission." In: International Conference on Rheology and Soil Mechanics: Proceedings, edited by M. J. Keedwell: 182–193: Spon Press. 1988.

Vallen, H. "Die Schallemissionsprüfung". Castell-Verlag GmbH, Wuppertal. 2003.